

High Harmonic Generation in SF₆: Raman-excited Vibrational Quantum Beats

Zachary B. Walters,¹ Stefano Tonzani,² and Chris H. Greene¹

¹*Department of Physics and JILA, University of Colorado, Boulder, Colorado 80309-0440, USA*

²*Department of Chemistry, Northwestern University, Evanston, Illinois 60208-3113, USA*

(Dated: September 25, 2018)

In a recent experiment (N. Wagner *et al.* [1]) on SF₆, a high-harmonic generating laser pulse is preceded by a pump pulse which stimulates Raman-active modes in the molecule. Varying the time delay between the two pulses modulates high harmonic intensity, with frequencies equal to the vibration frequencies of the Raman-active modes. We propose an explanation of this modulation as a quantum interference between competing pathways that occur via adjacent vibrational states of the molecule. The Raman and high harmonic processes act as beamsplitters, producing vibrational quantum beats among the Raman-active vibrational modes that are excited by the first pulse. We introduce a rigorous treatment of the electron-ion recombination process and the effect of the ionic Coulomb field in the electron propagation outside the molecule, improving over the widely-used three-step model.

PACS numbers:

High harmonic generation (HHG) is commonly understood as a 3 step process [2] in which an electron ionizes from a molecule, propagates in a strong laser field, and then recombines with the parent ion while emitting a photon. Acceleration by the laser field allows the electron to return with a large kinetic energy and emit photons with energy much higher than those of the driving laser.

Although the HHG process is primarily electronic in character, recent experiments have shown that vibrational degrees of freedom can play a role. In the experiment by Wagner *et al.*, [1] a 25 fs, 2.4×10^{14} W/cm² HHG laser pulse was preceded by a weaker 25 fs, 5×10^{13} W/cm² pulse which excited Raman-active vibrations in the molecule. The intensity of the high harmonic light was found to oscillate with the interpulse delay time at the excited molecular vibration frequencies. The surprising result was that the breathing mode, overwhelmingly dominant in conventional Raman experiments with this molecule, is no longer the strongest mode seen in the HHG experiment.

In this Letter, we interpret these oscillations as an interference between indistinguishable quantum pathways associated with different intermediate vibrational states during the HHG process, illustrated in Fig. 1. We develop a quantum mechanical description of the recent pump-probe SF₆ experiments, using a framework that substantially improves on the three-step model.[2] We have included the effects of the ion's Coulomb potential on the propagating electron, and utilized a nonperturbative electron-molecule scattering wavefunction [3] to calculate the recombination amplitude. The resulting calculation exhibits partial agreement with experimental observations.

We adopt a level of approximation in which all operators depending on the nuclear coordinates are expanded to first order in the normal mode coordinates Q_i ; then the full vibrational state vector $|\Psi(t)\rangle$ sepa-

rates into a product of uncoupled normal mode vectors $|\psi(t)\rangle^{(i)} = a_0^{(i)}(t)|0\rangle^{(i)} + a_1^{(i)}(t)|1\rangle^{(i)}$ that can be treated individually.

After a Raman pulse with the intensity and duration used in Ref.[1], only the $|0\rangle$ and $|1\rangle$ states of a given normal mode have significant amplitude. The following two-state, one-dimensional picture shows how individual Raman-active modes affect the high harmonic signal. Atomic units are used throughout this work.

During the Raman pulse, stimulated Raman scattering changes the vibrational state of the molecule from an initial $|0\rangle$ into a coherent superposition $a_0|0\rangle + a_1|1\rangle$ of the zeroth and first vibrational states. The vibrational coefficients follow equations of motion given by

$$i\dot{a}_{n_i}(t) = \omega_i \left(n_i + \frac{1}{2} \right) a_{n_i}(t) - \frac{1}{2} \sum_{A,B} E_A(t) E_B(t) \times \quad (1)$$

$$\left[\alpha_{AB} a_{n_i} + \partial_i \alpha_{AB} (\sqrt{n_i + 1} a_{n_i+1} + \sqrt{n_i} a_{n_i-1}) \right].$$

Here ω_i is the normal mode frequency, indices A and B run over $\{x, y, z\}$, $E_A(t)$ is the component of the electric field in the (body-frame) A direction at time t , Q_i is the normalized displacement associated with normal mode i and $\alpha_{AB}(Q_1, Q_2, \dots)$ is the polarizability tensor of the molecule. These equations of motion have off-diagonal elements only if $\partial_i \alpha_{AB} \equiv (2m\omega_i)^{-1/2} \partial \alpha_{AB} / \partial Q_i|_0 \neq 0$, which is the condition for a mode to be Raman active. The polarizability tensor and its derivatives are found by performing an unrestricted Hartree-Fock calculation [4] using the aug-cc-pVTZ basis set. [5]

Between laser pulses, $|0\rangle$ and $|1\rangle$ evolve as simple harmonic oscillator eigenstates, becoming $\psi_{\text{vib}} = a_0|0\rangle + a_1 e^{-i\omega\tau}|1\rangle$ at the beginning of the high harmonic pulse for an interpulse delay of τ , where the normal mode index (i) is omitted for brevity. Before the electron tunnels free of the ion, the high harmonic pulse stimulates the normal mode further according to Eq. (1). This is approximated

by a unitary 2×2 transfer matrix \underline{M} , where M_{nm} is the amplitude to end in state $|i\rangle$ after starting in state $|j\rangle$ at the beginning of the pulse.

Ionization and recombination, both electronic processes, are both modulated strongly by nuclear motion. Taylor-expanding the tunnel-ionization operator \hat{I} to first order in Q_i , with the substitutions $I_0 \hat{\mathbb{I}} \equiv I|_{\text{eq}}$ and $I_1^{(i)} \equiv (2m\omega_i)^{-1/2} \partial \hat{I} / \partial Q_i|_{\text{eq}}$ and the identity $Q_i = (2m\omega_i)^{-1/2} (\hat{A}_i + \hat{A}_i^\dagger)$, yields the first-order expansion into raising and lowering operators, $\hat{I} = I_0 \hat{\mathbb{I}} + \sum_i I_1^{(i)} (\hat{A}_i + \hat{A}_i^\dagger)$. Here $\hat{\mathbb{I}}$ is the identity operator, and $\hat{A}_i^\dagger, \hat{A}_i$ are the raising and lowering operators for the i -th normal mode. For each mode considered, the reduced mass m is equal to the mass of a single fluorine atom. The recombination operator \hat{R} can be derived to first order using identical logic. In both cases, dependence on nuclear positions means that the vibrational state changes along with the electronic state.

The evolution of the ionic vibrational/electronic wavefunction between ionization and recombination is in general quite complicated, since the three degenerate orbitals of SF_6^+ , which have T_{1g} symmetry, are coupled by vibrational degrees of freedom [6, 7, 8]. The linear and quadratic terms in the Jahn-Teller Hamiltonian [6, 7, 8], which governs the coupled vibrational/electronic evolution, are found for each Q_i by fitting the eigenvalues of the coupling matrix to the lowest 3 adiabatic energies of SF_6^+ for different displacements of the ion away from the maximum symmetry configuration. The energies are found using Gaussian's CASSCF method and a cc-PVDZ basis set[4]. In the notation of [6], $V_{T_{2g}} = .001209 \text{ H/bohr}$, $V_{E_g} = .1420 \text{ H/bohr}$, $N_1 = -.0362 \text{ H/bohr}^2$, $K_{T_{2g}} = .7288 \text{ H/bohr}^2$, $K_{E_g} = 1.8486 \text{ H/bohr}^2$. For the A_{1g} mode, which does not enter into the vibronic Hamiltonian, an adiabatic potential $E = V_{A_{1g}} Q_{A_{1g}} + 1/2 K_{A_{1g}} Q_{A_{1g}}^2$, with $V_{A_{1g}} = .0645 \text{ H/bohr}$, $K_{A_{1g}} = 2.98 \text{ H/bohr}^2$ gives the potential energy surface for all three electronic states. An important simplification is that the off-diagonal coupling between different electronic states, proportional to V_T , is small and can be neglected for the short times between ionization and recombination.

Neglecting off-diagonal coupling between electronic states, the adiabatic potential felt by the ion in a particular electronic state is $H_i = \frac{p_i^2}{2m} + V_i Q_i + \frac{1}{2} K_i Q_i^2$, which can be rewritten to first order in the basis of oscillator states of the neutral molecule. Evolution of the vibrational state is given by a transfer matrix $\underline{N} = \exp(-iH(t_{\text{ret}} - t_{\text{ion}}))$.

In a two-state treatment, the i -th vibrational wavefunction of the neutral molecule after recombination has occurred is $|\psi_{\text{vib}}\rangle = d_0 |0\rangle + d_1 |1\rangle$, where

$$\begin{pmatrix} \vec{d}_0 & \vec{d}_1 \end{pmatrix} = (a_0 \ a_1 e^{-i\omega\tau}) \underline{M}^T \underline{I}^T \underline{N}^T \underline{R}^T \quad (2)$$

and \underline{A}^T is the transpose of matrix \underline{A} .

The number of photons emitted in a given harmonic is proportional to $\vec{d}_0 \cdot \vec{d}_0^* + \vec{d}_1 \cdot \vec{d}_1^*$. The high harmonic intensity is a sum over all Raman active modes i :

$$P(\tau) = P_0 + \sum_i P_1^{(i)} \cos(\omega_i \tau + \delta_i) \quad (3)$$

The static P_0 primarily results from terms of the form $a_0^* a_0$, while P_1 results from terms of the form $a_0 a_1^* e^{i\omega\tau}$ and $a_1 a_0^* e^{-i\omega\tau}$. Defining $\underline{W} = \underline{M}^\dagger \underline{I}^\dagger \underline{N}^\dagger \underline{R}^\dagger \cdot \underline{R} \underline{N} \underline{I} \underline{M}$, $P_0 = a_0^* W_{00} a_0^*$ and $P_1 \cos(\omega t + \delta) = \frac{1}{2} (a_1^* e^{i\omega\tau} W_{10} a_0 + \text{c.c.})$. Since I_1 and R_1 are small relative to I_0 and R_0 , only their first-order terms are kept.

At this level of approximation, calculating \hat{I} and \hat{R} as functions of the nuclear coordinates and substituting the expectation values for Q_i at ionization and recombination would give identical results. Nevertheless, tracking the quantum mechanical pathways in this manner is informative, because it allows the prediction of other observables less amenable to a ‘‘classical nuclear motion’’ analysis, like the relative populations in $|0\rangle$ or $|1\rangle$ after recombination.

This framework is applied to real molecules, using an improved version of the 3 step model. For the ionization step, a simple one-dimensional WKB tunneling picture describes an electron tunneling only in directions parallel to the laser electric field. This is motivated by the ‘‘initial value representation’’ [9, 10]. In the classically forbidden region under the barrier formed by the molecular potential and the laser field, the tunneling wavefunction equals the value of the unperturbed molecular HOMO at the inner turning point times a declining WKB exponential. With the direction of the electric field as $-\hat{z}$, the wavefunction at the outer and inner turning points are related by

$$\psi_t(x, y, z_{\text{tp2}}, t) = \psi_{\text{HOMO}}(x, y, z_{\text{tp1}}, t) \times |C_1/C_2|^{1/6} \text{Bi}(0)/\text{Ai}(0) \exp\left[-\int_{z_{\text{tp1}}}^{z_{\text{tp2}}} dz k(z)\right], \quad (4)$$

where $k(z) = \sqrt{2(V_{\text{mol}} + V_{\text{laser}} - E)}$, Ai and Bi are Airy functions, z_{tp1} and z_{tp2} are the inner and outer turning points, C_1 and C_2 are the z components of the slopes of $2V(\vec{r}, t)$ at the two turning points, and the path integral is calculated along the z direction parallel to the applied electric field.

After tunneling, the free electron wavefunction's evolution is relatively simple until it rescatters from the parent ion. $\psi_c(r, \Omega, t)$, the continuum wavefunction at the instant just prior to the electron rescattering from the molecular ion, is found using Gutzwiller's semiclassical propagator [11]:

$$K(\vec{r}, t; \vec{r}_0, t_0) = (2\pi i)^{-3/2} \sqrt{C(\vec{r}, t; \vec{r}_0, t_0)} \times \exp[iS(\vec{r}, t; \vec{r}_0, t_0) - i\phi] \quad (5)$$

Here $S(\vec{r}, t; \vec{r}_0, t_0)$ is the action integral $S = \int L(q, \dot{q}, t) dt$ calculated for the classical trajectory starting at (\vec{r}, t) and

ending at (\vec{r}_0, t_0) and $C(\vec{r}, t; \vec{r}_0, t_0) = |-\frac{\partial^2 S}{\partial r_{0,A} \partial r_B}|$ is the density of trajectories for given initial and final points. ϕ is a phase factor equal to $\frac{\pi}{2}$ times the number of conjugate points crossed by the trajectory. The semiclassical continuum wavefunction is

$$\psi_c(\vec{r}, t) = \int d^3\vec{r}_0 \int dt_0 K(\vec{r}, t; \vec{r}_0, t_0) \psi_t(\vec{r}_0, t_0) \quad (6)$$

When the electron recollides with the parent ion, its wavefunction is distorted strongly by the molecular potential and by exchange effects with the other electrons, which can dramatically change amplitudes for recombination with respect to the plane wave approximation. Techniques described in Refs [3, 12, 13] determine a complete set of stationary field-free electron-molecule scattering states. Beyond the range of the molecular potential, the scattering states are given in terms of incoming and outgoing Coulomb radial functions $f_{El}^\pm(r)$ and the scattering S-matrix as

$$\begin{aligned} \psi_{E,lm}(\vec{r}) &= \frac{1}{i\sqrt{2}} f_{El}^-(r) Y_{l,m}(\theta, \phi) - \\ &\frac{1}{i\sqrt{2}} \sum_{l',m'} f_{El'}^+(r) Y_{l',m'}(\theta, \phi) S_{l',m';l,m}(E). \end{aligned} \quad (7)$$

During the electron-molecule scattering, when recombination occurs, the electron wavepacket is expanded in terms of these scattering states as $\psi_S = \int dE \sum_{l,m} A_{l,m}(E) \psi_{E,lm} e^{-iEt}$, where

$$A_{l,m}(E) = e^{iEt} \int d^3\vec{r} \psi_{E,lm}^*(\vec{r}) \psi_c(\vec{r}, t). \quad (8)$$

For a chosen time of projection onto the scattering states, Eqs. (6) and (8) together define a seven-dimensional integral over initial and final positions and initial times. However, the integrand oscillates rapidly almost everywhere, causing cancellations. Stationary phase techniques identify the region where the integrand oscillates slowly, which permits evaluation.

The semiclassical action S is expanded to second order around the starting and ending points of some classical trajectory, and about the starting time. Near the starting position and time, $\psi_t(\vec{r}_0 + \delta\vec{r}_0, t_0 + \delta t_0) = \psi_t(\vec{r}_0, t_0) \exp[i(\vec{k}_0 \delta\vec{r}_0 - iE_{\text{HOMO}} \delta t_0)]$, while $f_{E,l}^\pm(r + \delta r) = f_{E,l}(r) \exp[\mp i k_{E,l}(r) \delta r]$, where $k_{E,l}(r) = \sqrt{2(E - V_l(r))}$, near the final position. Angular derivatives of the spherical harmonics are neglected.

The integrand oscillates most slowly when its complex phase is nearly constant. This happens when the linear terms in the S expansion are canceled by the linear terms in the complex phases of the initial and final states. For such a trajectory, the contributions of nearby trajectories with nearly the same $\vec{x}_0, t_0, \vec{x}, t$ to the integral will tend to add constructively. These “stationary phase” trajectories are not the only trajectories of interest in the problem, but expanding S about their beginning and ending

points describes the phase in the slowly-varying region of interest.

These stationary phase conditions are met by a trajectory that begins “downstream” of the molecule in the direction of the electric field with zero momentum, moves only radially and parallel to the electric field until it reencounters the parent molecule at the scattering state energy. Only the incoming-wave part of the scattering states gives a nonvanishing contribution to the expansion coefficients. Performing the resulting gaussian integrals about the initial and final points, and about the initial time, yields expansion coefficients

$$A_{l,m}(E) = \frac{4\pi^2}{i\sqrt{2}} \sqrt{\left| \frac{\partial r_A}{\partial p_{0,B}} \right|} \left(\frac{\partial H}{\partial t_0} \right)^{-\frac{1}{2}} f_{El}^-(r) Y_{l,m}^*(\hat{z}) e^{i[S(\vec{r}, t, \vec{r}_0, t_0) - \phi]} \psi_t(\vec{r}_0) e^{[-iE_{\text{HOMO}} t_0]} \quad (9)$$

for a stationary phase trajectory that starts at (z_0, t_0) and ends at (z, t) , where \hat{z} is the direction of the electric field at the time of ionization.

The recombination amplitude is now $\vec{D}(E) = \sum_{l,m} A_{l,m}(E) \vec{d}_{l,m}(E)$, where $\vec{d}_{l,m} = \langle \psi_g | \vec{x} | \psi_{E,lm} \rangle$ is the recombination amplitude calculated for each individual scattering state. This connects to the quantum paths framework when $I = \psi_t(\vec{r}_0, t_0)$, and $\vec{R} = \vec{D}(E)$ calculated for $I = 1$. Both quantities are calculated at the equilibrium geometry, then for a geometry distorted by 0.1 bohr in the normal mode coordinate to find \hat{I}, \hat{R} and their derivatives. This involves recalculating the scattering states and recombination dipoles for the distorted geometry.

The modulation of the 39th harmonic, which the JILA experiment considered in detail, is calculated for comparison with experiment. This harmonic is close to the measured cutoff, so it can only be produced by a laser half-cycle where the maximum of the electric field falls close to the maximum of the Gaussian envelope. Accordingly, only the modulation for a single half-cycle where these two maxima coincide was used. In the expression for the harmonic intensity at some harmonic order, Eq. (3), all the quantities depend on molecular orientation. A rotational average of P_0 and P_1 were calculated, since the JILA experiment was performed on a gas jet of molecules which had no preferred orientation. Only polarizations perpendicular to the propagating beam were included in these averages. Although each of the T_{2g} and E_g modes modulates the harmonic intensity strongly at particular orientations, the phase offset δ in $P_1 \cos(\omega\tau + \delta)$ changes with orientation, cancelling some of the observed oscillation. The more symmetric A_g mode experiences less cancellation because the initial Raman pulse stimulates it equally for all molecular orientations. The trends in the peak intensities of different normal modes are, however, similar with and without the phase. Fig. 2 compares the spherically averaged peak-to-peak modulation with phase information included, with phase information

excluded by setting $\delta = 0$ for all orientations, and the experimentally measured modulations for each mode for the two runs for which all three mode modulations could be distinguished from the background [14]. It should be noted that although the relative peak intensities are not in agreement with experiment, the intensities for the different peaks are all the same order of magnitude, whereas in the Raman spectrum the A_g mode is 20 times more intense than the others. [1]

Since the scattering wavefunction is expanded in field-free scattering states, the calculated modulation varies slightly depending on the time at which the semiclassical wavefunction is projected onto the scattering states. Additional uncertainty may arise because of the various approximations made in the treatment of molecular scattering, detailed in [3, 12, 13]. Fig. 2 shows modulations calculated when this projection is made at $\omega t = 3.9$ radians, when the short electron trajectories return to the vicinity of the parent molecule with the correct energy to yield 39th harmonic photons upon recombination.

In the present work, we have combined for the first time a rigorous treatment of electron-molecule scattering with a semiclassical description of electronic propagation, resulting in a flexible and robust implementation that has been used to treat a complex molecule with many internal degrees of freedom to a level of sophistication that is unprecedented in this area of research for such a large system. We have shown how the internal degrees of freedom allow for phenomena which have no analogue in atomic systems, demonstrating that the HHG signal can be modulated interferometrically by a molecule's vibrational state. Thus HHG could serve both as an interferometric probe of chemical dynamics (similar to the way in which rearrangement dynamics are investigated in Ref. [15]) and as a complementary tool to traditional spectroscopic techniques, offering great potential for future investigations.

Acknowledgments: The authors would like to thank N. Wagner, A. Wüest, M. Murnane, and H. Kapteyn for many stimulating discussions. This work was supported in part by the Department of Energy, Office of Science, and in part by the NSF EUV Engineering Research Center.

-
- [1] N. L. Wagner, A. Wuest, I. P. Christov, T. Popmintchev, X. Zhou, M. M. Murnane, and H. C. Kapteyn, Proc. Natl. Acad. Sci. U.S.A. **103**, 13279 (2006).
 - [2] M. Lewenstein, P. Balcou, M.Y. Ivanov, A. L'Huillier, and P.B. Corkum, Phys. Rev. A **49**, 2117 (1994).
 - [3] S. Tonzani and C. H. Greene, J. Chem. Phys. **122**, 014111 (2005).
 - [4] M. J. F. et al, Gaussian Inc., Pittsburgh, PA (1998).
 - [5] T. Dunning, J. Chem. Phys p. 1007 (1989).
 - [6] S. Estreicher and T. L. Estle, Phys. Rev. B **31**, 5616

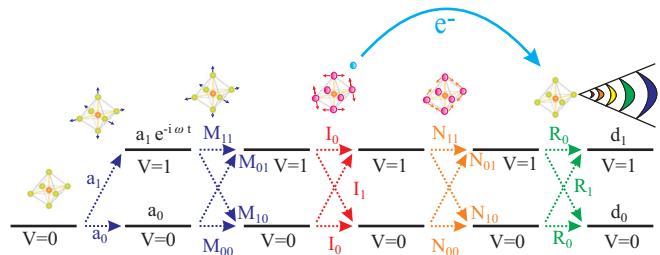


FIG. 1: (Color online) The vibrational interference model in one dimension. The molecule ends the Raman pulse in a superposition of the $v=0$ and $v=1$ vibrational states. After a time delay, the two vibrational states are mixed by stimulated Raman scattering, “hopping” during ionization and recombination, and evolution of the ionic wavefunction while the electron is away. Interference between adjacent vibrational states modulates the high harmonic signal.

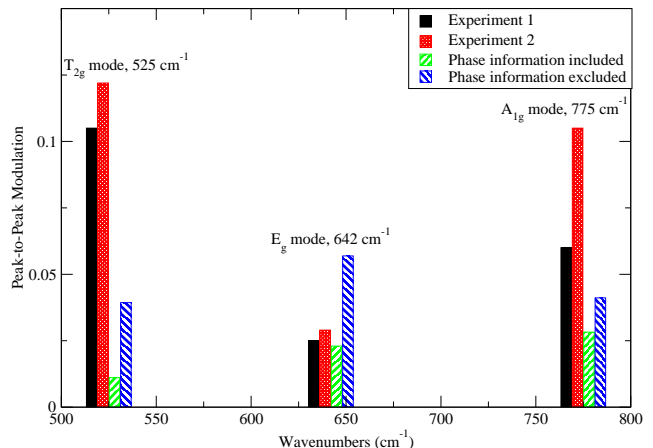


FIG. 2: (Color online) Peak-to-peak modulation of the high harmonic signal vs. wavenumber, comparing theory to the two experimental runs for which data is available. Modulations corresponding to the same frequency have been placed side-to-side for purpose of comparison.

- (1985).
- [7] W. Moffitt and W. Thorson, Phys. Rev. **108**, 1251 (1957).
- [8] I. Bersuker, *The Jahn-Teller effect and vibronic interactions in modern chemistry* (Plenum Press, 1984).
- [9] W. H. Miller, J. Phys. Chem. A **105**, 2942 (2001).
- [10] H. Nakamura, J. Theor. Comp. Chem. **4**, 127 (2005).
- [11] M. C. Gutzwiller, *Chaos in Classical and Quantum Mechanics* (Springer, New York, 1990).
- [12] S. Tonzani and C. H. Greene, J. Chem. Phys. **124**, 054312 (2006).
- [13] S. Tonzani, Comp. Phys. Comm. **176**, 146 (2007).
- [14] N. Wagner, private communication.
- [15] S. Baker, J. S. Robinson, C. A. Haworth, H. Teng, R. A. Smith, C. C. Chirila, M. Lein, J. W. G. Tisch, and J. P. Marangos, Science **312**, 424 (2006).